

Time-Dependent Migration of Systemically Delivered Bone Marrow Mesenchymal Stem Cells to the Infarcted Heart

Ana Carolina M. Assis,* Juliana L. Carvalho,† Bruno A. Jacoby,*
Raphael L. B. Ferreira,‡ Paula Castanheira,† Simone O. F. Diniz,‡
Valbert N. Cardoso,‡ Alfredo M. Goes,† and Anderson J. Ferreira*

*Department of Morphology, Biological Sciences Institute,
Federal University of Minas Gerais, Belo Horizonte, MG, Brazil

†Department of Biochemistry and Immunology, Biological Sciences Institute,
Federal University of Minas Gerais, Belo Horizonte, MG, Brazil

‡Department of Clinical and Toxicological Analysis, Pharmacy Faculty,
Federal University of Minas Gerais, Belo Horizonte, MG, Brazil

In this study the time course of homing and the body distribution of systemically delivered bone marrow mesenchymal stem cells (BM-MSCs) after myocardial infarction (MI) were evaluated. BM-MSCs were isolated from Wistar rats, expanded in vitro, and their phenotypical characterization was performed by flow cytometer. Rats were randomly divided into three groups: control, sham MI, and MI. BM-MSCs (5×10^6) were labeled with ^{99m}Tc -HMPAO and injected through the tail vein 7 days after MI. Gamma camera imaging was performed at 5, 15, 30, and 60 min after cell inoculation. Due to the ^{99m}Tc short half-life, cell migration and location were also evaluated in heart sections using DAPI-labeled cells 7 days after transplantation. Phenotypical characterization showed that BM-MSCs were CD90⁺, CD73⁺, CD54⁺, and CD45⁻. Five minutes after ^{99m}Tc -HMPAO-labeled cell injection, they were detected in various tissues. The cells migrated mainly to the lungs (approximately 70%) and, in small amounts, to the heart, kidneys, spleen, and bladder. The number of cells in the heart and lungs decreased after 60 min. MI markedly increased the amount of cells in the heart, but not in the lungs, during the period of observation (4.55 ± 0.32 vs. $6.34 \pm 0.67\%$ of uptake in infarcted hearts). No significant differences were observed between control and sham groups. Additionally, 7 days after DAPI-labeled cells injection, they were still detected in the heart but only in infarcted areas. These results suggest that the migration of systemically delivered BM-MSCs to the heart is time dependent and MI specifically increases BM-MSCs homing to injured hearts. However, the systemic delivery is limited by cell entrapment in the lungs.

Key words: Myocardial infarction; Mesenchymal stem cells; Homing; Body distribution

INTRODUCTION

Mesenchymal stem cells (MSCs) have been isolated from multiple adult tissue sources, such as cord blood, placenta, adipose and dermal tissues, synovial fluid, deciduous teeth, and amniotic fluid (19). This broad distribution of sources combined with their ability to differentiate into multiple mesenchymal phenotypes, such as bone, cartilage, tendon, and adipose tissue, has led them to be referred as potential therapeutic candidates for several diseases and degenerative processes, including myocardial infarction (MI) (18,37). In addition to these MSCs sources, it is well documented that bone marrow contains cells usually called bone marrow mesenchymal

stem cells (BM-MSCs) that can differentiate into different cellular types (5,14,27).

Many reports have shown that cellular therapy using BM-MSCs is able to improve cardiac function after myocardial ischemia in different species, including humans (2,30). However, the mechanisms by which BM-MSCs induce their beneficial effects in the heart are still controversial. Thus, it has been proposed that BM-MSCs can differentiate into both vascular endothelial cells and cardiomyocytes, activate local factors, fuse with resident cells, or even a combination of these mechanisms that ultimately lead to a restoration of the cardiac structure and function (6,7,32).

A critical point for the clinical success of stem cell-

Received November 24, 2008; final acceptance October 30, 2009. Online prepub date: November 10, 2009.

Address correspondence to Anderson J. Ferreira, Ph.D., Department of Morphology, Av. Antônio Carlos, 6627-ICB, UFMG, 31 270-901, Belo Horizonte, MG, Brazil. Tel: (55-31)3409-2811; Fax: (55-31)3409-2810; E-mail: anderson@icb.ufmg.br

based therapy for myocardial repair is an efficient method for cell delivery. Previous studies have demonstrated that BM-MSCs intracoronarily, intravenously, and directly injected into the infarcted heart promote tissue regeneration (10,33). Intravenous injection of BM-MSCs constitutes an attractive noninvasive strategy because it allows repeated administration of large numbers of cells. Therefore, it has been reported that systemically delivered BM-MSCs is a feasible strategy to reverse, at least partially, the damage induced by MI (17,29,34). However, data regarding the BM-MSCs kinetic and body distribution during the first hour after intravenous injection are still missing. Thus, the purpose of the current study was to evaluate the time course of homing and the body distribution of systemically delivered BM-MSCs after MI in rats.

MATERIALS AND METHODS

Animals

Female Wistar rats weighting 200–250 g ($n = 4-8$) were obtained from the animal facility at the Federal University of Minas Gerais (CEBIO, Brazil). The animals were housed in a climate-controlled environment under a 12-h light/dark cycle with free access to rat chow and water. All experimental protocols were performed in accordance with the guidelines for the humane use of laboratory animals established at our Institution (Protocol #152/2006).

BM-MSCs Isolation and Culture

BM-MSCs were obtained from 4-week-old rats. Bone marrow was flushed out from tibias and femurs using DMEM medium and centrifuged at 1,400 rpm for 10 min. The cells were resuspended in DMEM supplemented with 10% fetal bovine serum and plated in T75 tissue culture flasks (Techno Plastic Products, Switzerland). The cultures were kept in a humidified atmosphere with 5% CO₂ at 37°C for 3 days before the first medium change. The mesenchymal population was isolated based on their ability to adhere on the culture plate. At 90% confluence, the cells were detached with 0.25% trypsin-EDTA (Sigma-Aldrich, USA) and replated in other flasks at 1:3 ratios. Third passage BM-MSCs were used in all experiments (24,26).

Phenotypical Characterization of BM-MSCs

The adherent cells were detached with 0.25% trypsin/EDTA, centrifuged for 5 min at $1,200 \times g$, and resuspended in PBS. Aliquots containing 5×10^5 cells were incubated with monoclonal primary antibodies specific for CD45, CD73, CD54, and CD90 (BD Pharmingen, USA) for 30 min at 4°C. The cells were washed and incubated with the secondary antibody, IgG anti-mouse Alexa 488-conjugated (Invitrogen, USA), for an addi-

tional 30 min at 4°C. Alexa 488-conjugated isotype-identical IgG served as negative control. Finally, the cells were fixed in 10% formalin and analyzed using a FACScan (BD Immunocytometry System, USA). For each sample, 20,000 events were acquired and analyzed using the CELL QUEST software. Cell surface marker expression was determined by comparison with isotype control on a histogram plot and data analysis was performed using WinMid 2.8 analysis software.

Alkaline Phosphatase Activity

Alkaline phosphatase activity was evaluated by the NBT-BCIP assay (GIBCO®, Invitrogen Cell Culture, USA), according to Machado et al. (20). The cells (2×10^5 cells/well) were seeded in 24-well plates and the BCIP-NBT solution (210 µl), prepared according to the manufacturer's instructions, was added to each well after completely removal of the culture medium from the BM-MSCs cultures. Two hours after incubation at 37°C in a humidified 5% CO₂, the cells were observed by optical microscopy and the presence of insoluble purple precipitates were evaluated.

Cellular Viability Assay

The viability of the cells was evaluated by the 3-(4,5-dimethylthiazol-2-yl)-2,5-diphenyl tetrazolium bromide (MTT) assay (4,13,15,23). The cells (2×10^5 cells/well) were seeded in 24-well plates. Briefly, 170 µl of MTT (5 mg/ml; Sigma-Aldrich, USA) were added to each well and incubated in a humidified 5% CO₂ atmosphere at 37°C. Two hours later, the cell morphology and presence of formazan salts were visualized in an inverted optical microscope.

Myocardial Infarction Procedures

MI was performed according to Ferreira et al. (12). Under anesthesia with 10% ketamine/2% xylazine (4:3, 0.1 ml/100 g, IP), the rats were placed in the supine position on a surgical table, tracheotomized, intubated, and ventilated with room air using a respirator for small rodents. Subdermal electrodes were placed to allow the electrocardiogram (ECG) recordings. The chest was opened by a left thoracotomy at the fourth or fifth intercostal space. To expose the heart, a small-sized retractor was used to maintain the ribs separated. After incision of the pericardium, the heart was quickly removed from the thoracic cavity and turned left to allow access to the proximal left anterior descending (LAD) coronary artery. A 4-0 silk suture was snared around the LAD coronary artery and tightly ligated to occlude the vessel. The heart was then placed back and the chest was closed with 4-0 silk sutures. Sham-operated rats were treated in the same manner, but the coronary artery was not ligated. After surgical procedures, ECG tracings were ob-

tained in order to confirm the myocardial ischemia. Seven days after the surgery, MI was confirmed by Masson's trichrome staining and by nuclear imaging using ^{99m}Tc -SESTAMIBI (Cardiolite®, Bristol-Myers Squibb Medical Imaging, Inc., USA).

Cell Labeling and Injection

The BM-MSCs were labeled with technetium- ^{99m}Tc by incubation with ^{99m}Tc -*d,l*-hexamethylpropylene amine oxime (HMPAO) (Ceretek®; Amersham Healthcare, USA) (18,22). ^{99m}Tc -HMPAO complex (370 MBq) diluted in saline (5 ml) was slowly added to the BM-MSCs suspension and incubated for 15 min at 37°C. After labeling, the radiochemical purity of the ^{99m}Tc -HMPAO was determined by partition between 0.9% saline and chloroform (3). A cell suspension with approximately 5×10^6 cells containing 37 MBq was used for each experiment.

Because ^{99m}Tc has a short half-life (approximately 6 h), cell migration and location were also evaluated using 4',6-diamidino-2-phenylindole (DAPI)-labeled cells 7 days after transplantation. In brief, sterile DAPI stock solution (Sigma-Aldrich, USA) was added to the culture medium at the day of transplantation at a final concentration of 50 µg/ml for 2 h. After incorporation of the DAPI into the nuclei, cells were rinsed six times in PBS to remove unbound DAPI, detached with 0.25% trypsin-EDTA, and resuspended in saline for cell transplantation. Using this protocol, the level of expression of DAPI in the MSCs is approximately 100% (25).

For cell injection, the rats were anesthetized with 10% ketamine/2% xylazine (4:3, 0.1 ml/100 g, IP) and ^{99m}Tc -HMPAO or DAPI-labeled BM-MSCs (5×10^6) suspended in 100 µl of saline were injected through the tail vein 7 days after MI. The ^{99m}Tc -HMPAO-injected animals were divided into three groups: control (no surgery plus BM-MSCs), MI plus BM-MSCs, and sham MI plus BM-MSCs. Because no significant differences were observed between control and sham-operated animals, these two groups were combined. Considering that it is impossible to inject the whole radioactive content of the syringe used to inoculate the cells, the emission of radioactivity from the syringe was measured before and after the injection in order to normalize the gamma camera results.

Scintigraphic Imaging and Counting

Scintigraphic images were obtained by gamma camera equipped with a low-energy collimator (Nuclide TH 22, Mediso, Hungary) at 5, 15, 30, and 60 min after the ^{99m}Tc -HMPAO-labeled BM-MSC injection. Five-minute static planar images were acquired using a 256×256 -pixel matrix. The scintigrams were analyzed in the regions of interest (ROI) to specific organs. In order to

determine the percentage of the infused cells in each organ, the uptake was calculated as a percentage of the total counting obtained in all organs analyzed.

Biodistribution Studies

Because the radioactivity from heart and lungs could overlap due to the close localization of these two organs, an additional group of rats was killed 60 min after cell injection and heart, lungs, kidneys, spleen, and bladder were collected. The individual radioactivity from each organ was counted using a gamma counter with NaI (TI) crystal (ANSR, Abbot, Chicago, USA) and the results were normalized by the organ weights. The uptake percentage to each organ was calculated by the following formula (cpm: counts per minute): % uptake = [cpm/organ weight (g) \times 100]/[sum of cpm/weight of all organs (g)].

Histological Analysis

Seven days after DAPI-labeled BM-MSCs infusion ($n = 3$), the rats were killed, and their hearts were excised and washed with 100 ml of saline through the aorta artery. For fixation, the hearts were perfused fixed with PBS and dimethyl sulfoxide (DMSO). At the end of perfusion, the hearts were kept in 80% methanol/20% DMSO fixative for 6 days at -80°C followed by 24 h at -20°C . The tissues were dehydrated by sequential washes with 100% ethanol and xylene and then imbedded in paraffin. Transversal sections (6 µm) were cut starting from the base area of the heart at intervals of 40 µm. Sections were mounted on slides and DAPI-labeled cells were directly observed under confocal microscopy.

Statistical Analysis

All data are expressed as mean \pm SEM. Statistical analysis was performed using two-way ANOVA followed by the Bonferroni test or Student *t*-test (Prism 4.0 Graphpad software, Inc.). Statistical significance was accepted at $p < 0.05$ and a power of the test $\geq 80\%$.

RESULTS

BM-MSCs Characterization

The ability of the BM-MSCs to adhere on culture flasks is one of their characteristics utilized to identify these cells. In this study we used this property to isolate them from other bone marrow cells such as hematopoietic and fibroblastic cells, which constitute the majority of cells in the bone marrow. Nonadherent cells were easily removed from cultures with subsequent medium changes. Four days after collection and culture of bone marrow cells, BM-MSCs were adhered on the flasks, forming small colonies with fibroblast-shaped morphology. After 2 weeks, the adherent cells reached approximately 90% confluence and they were reseeded for the first time. The fibroblast-like morphology was main-

tained after all cell passages and throughout the experimental period.

After the third passage, BM-MSCs were phenotypically characterized by flow cytometry using panels of antibodies. Because 97% of the cells did not express CD45 and 86%, 94%, and 95% of the cells expressed CD90, CD73, and CD54, respectively, we characterized these cells as CD90⁺, CD73⁺, CD54⁺, and CD45⁻ (Fig. 1A). In addition, the activity of alkaline phosphatase in BM-MSCs was evaluated by NBT-BCIP assay and the presence of insoluble purple precipitates is shown in Figure 1B, indicating that the cells were activated and excluding any contamination with fibroblasts. Finally, the cellular viability was assessed by the MTT assay. The formation of formazan salts in the cell cultures, as observed in Figure 1C, indicates that the cells are viable. Together these findings show that more than 90% of the isolated cells correspond to activated and viable BM-MSCs. The labeling yield of the BM-MSCs with the lipophilic complex (^{99m}Tc-HMPAO) was approximately of 60%.

Myocardial Infarction

MI was confirmed immediately after surgical procedures by ECG. Also, 7 days after surgeries, MI was confirmed by Masson's trichrome staining and by myocardial perfusion scintigraphic imaging. ECG tracings from infarcted rats showed an elevation of the ST segment and an increase in the R wave amplitude (Fig. 2A). Scintigraphic imaging showed hypocaptation of the tracer which suggested the presence of a perfusion deficit localized in the territory supplied by the LAD coronary artery (Fig. 2B). In addition, the presence of infarcted area was visualized by Masson's trichrome staining (Fig. 2C). These observations are consistent with the MI model generated by the LAD coronary artery ligation.

Scintigraphic Imaging and Counting

Scintigraphic images obtained 5 min after injection of ^{99m}Tc-HMPAO-labeled BM-MSCs showed radioactivity uptake in various tissues (Fig. 3A). The cells migrated mainly to the lungs (approximately 70%) and, in small amounts, to the heart, kidneys, bladder, and spleen in control and MI rats (Fig. 3B). At the first time point analyzed (5 min), the number of cells that migrated to the heart of infarcted rats was significantly higher when compared with sham-operated animals ($p < 0.05$ and power of the test = 95.8%). Furthermore, the amount of ^{99m}Tc-BM-MSCs in the heart and in the right lung decreased at 60 min of injection in infarcted animals (heart: $8.2 \pm 0.7\%$ uptake at 5 min vs. $4.5 \pm 1.2\%$ uptake at 60 min after cell injection, $p < 0.05$ and power of the test = 80.3%) (Fig. 4). In contrast, it was observed a markedly increase in the radioactivity from the bladder

of infarcted rats. The number of BM-MSCs in organs of control rats did not change significantly after 60 min of injection (Fig. 4). As observed in Figure 5, MI procedure increased the uptake of radiolabeled cells in the heart during the period of observation (average: 4.5 ± 0.3 vs. $6.0 \pm 0.8\%$ uptake in infarcted hearts, $p < 0.05$). This effect was apparently specific to the injured tissue because no significant changes were observed in other organs.

Biodistribution of BM-MSCs

It is pertinent to suppose that, during the imaging procedure, the radioactivity from heart and lungs could overlap due to the close localization of these two organs. Thus, we used an additional group of rats to analyze the specific radioactivity of isolated hearts and lungs after 60 min of BM-MSCs infusion. In keeping with the whole body imaging findings, the biodistribution results showed that the radioactivity from infarcted hearts was 23-fold higher than control hearts. In addition, only a discrete increase in the radioactivity from lungs (1.3-fold) was observed.

Finally, after 7 days of DAPI-labeled cell injection, the cells were still detected in the heart and restricted to the infarcted areas (Fig. 6).

DISCUSSION

In the current study, using a radioactive tracing technique, we evaluated the time course of homing and the body distribution of systemically delivered BM-MSCs 7 days after MI. The most significant findings of this study are that at the minimal time point analyzed (i.e., 5 min after cell injection) BM-MSCs were detected in various organs and the amount of cells in infarcted hearts was significantly higher compared with sham-operated rats ($p < 0.05$ and power of the test = 95.8%). However, at 60 min of injection, the amount of BM-MSCs in infarcted hearts returned to the control levels. In addition, independently of the cardiac injury, the majority of the inoculated cells were localized in the lungs, suggesting that cell entrapment in this organ is a limiting factor for cell delivery using the intravenous route.

The quantification of cell lodging is a prerequisite for any analysis of homing mechanism, especially in vivo. Leukocyte ^{99m}Tc-HMPAO labeling is a widely used technique for detection of inflammation and infection focus (22). Only recently it has been achieving an important role in stem cell labeling, allowing the evaluation of their behavior in vivo for as long as 18–24 h after injection. BM-MSCs can be labeled using ^{99m}Tc-HMPAO without affecting their viability and preserving their ability of adhesion and proliferation in in vitro cultures (21,35). In the present study we have successfully used this technique to monitor the body distribution of

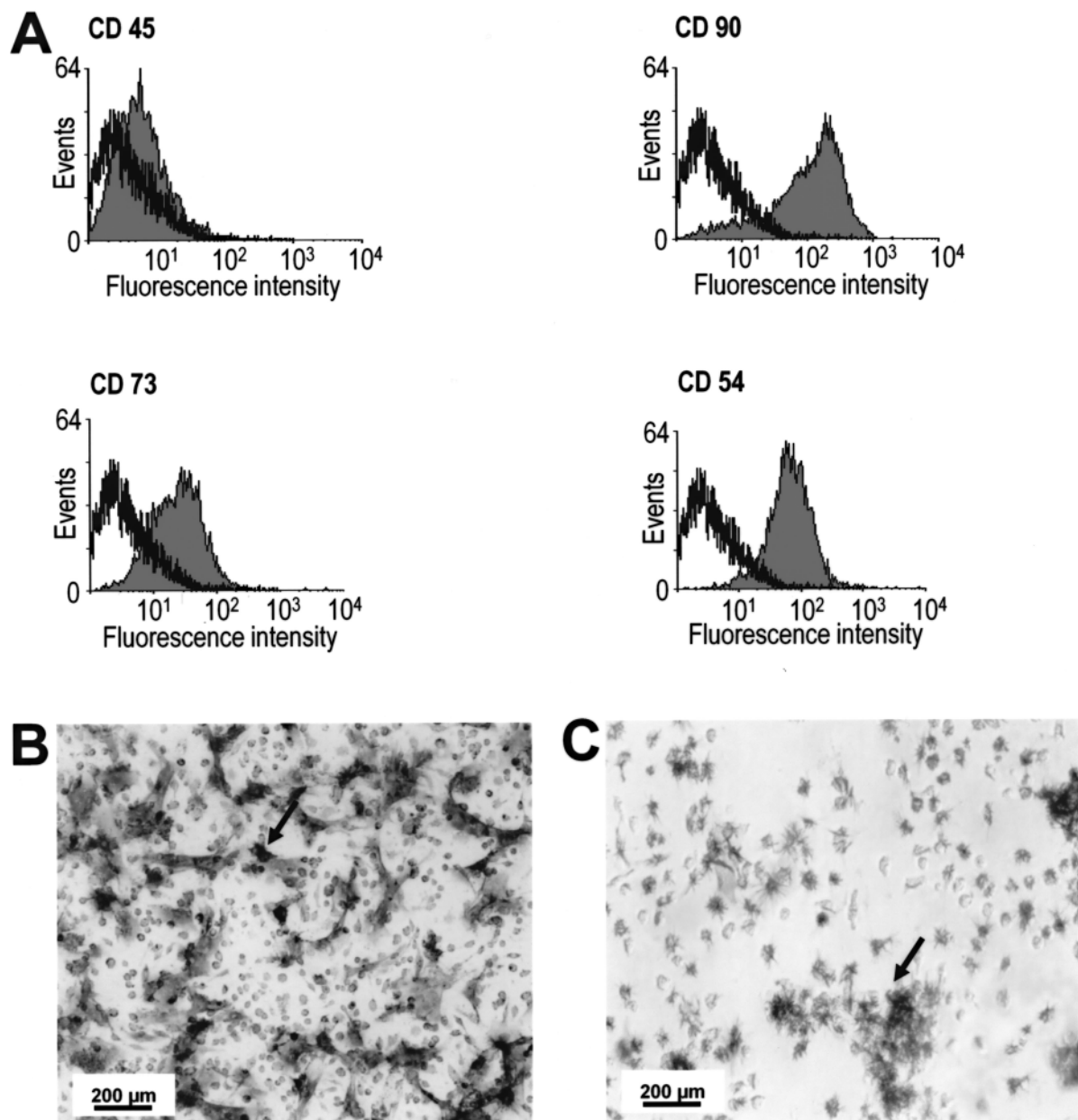


Figure 1. Phenotypic characterization of BM-MSCs. (A) The graphs show the expression profile of BM-MSCs surface markers. Flow cytometry revealed that the cells are CD90⁺, CD73⁺, CD54⁺, and CD45⁻. The black line represents the fluorescence obtained in negative control. Points at the left of the black line are considered negative. Gray region constitutes the fluorescence values obtained from the analyzed population of cells. (B) Visualization of insoluble precipitates (arrow) by optical microscopy in the NBT-BCIP assay indicating alkaline phosphatase activity. (C) Visualization of formazan crystals (arrow) by optical microscopy in the MTT assay. The formation of crystals indicates the presence of viable cells.

systemically delivered BM-MSCs labeled with ^{99m}Tc-HMPAO in a model of MI in rats.

We employed a simple technique based on the ability of the BM-MSCs to adhere to the culture flasks to isolate them from other bone marrow cells. The BM-MSCs identity was confirmed by flow cytometry analysis, which showed that these cells are CD90⁺, CD73⁺, and

CD54⁺ but CD45⁻ (6,8,11). Thus, in addition to their fibroblast-shaped morphology, it was possible to conclude that the cell population used in our study was an enriched culture of BM-MSCs. Furthermore, the activated state of the cells as well as their viability was confirmed by the alkaline phosphatase and the MTT assays, respectively.

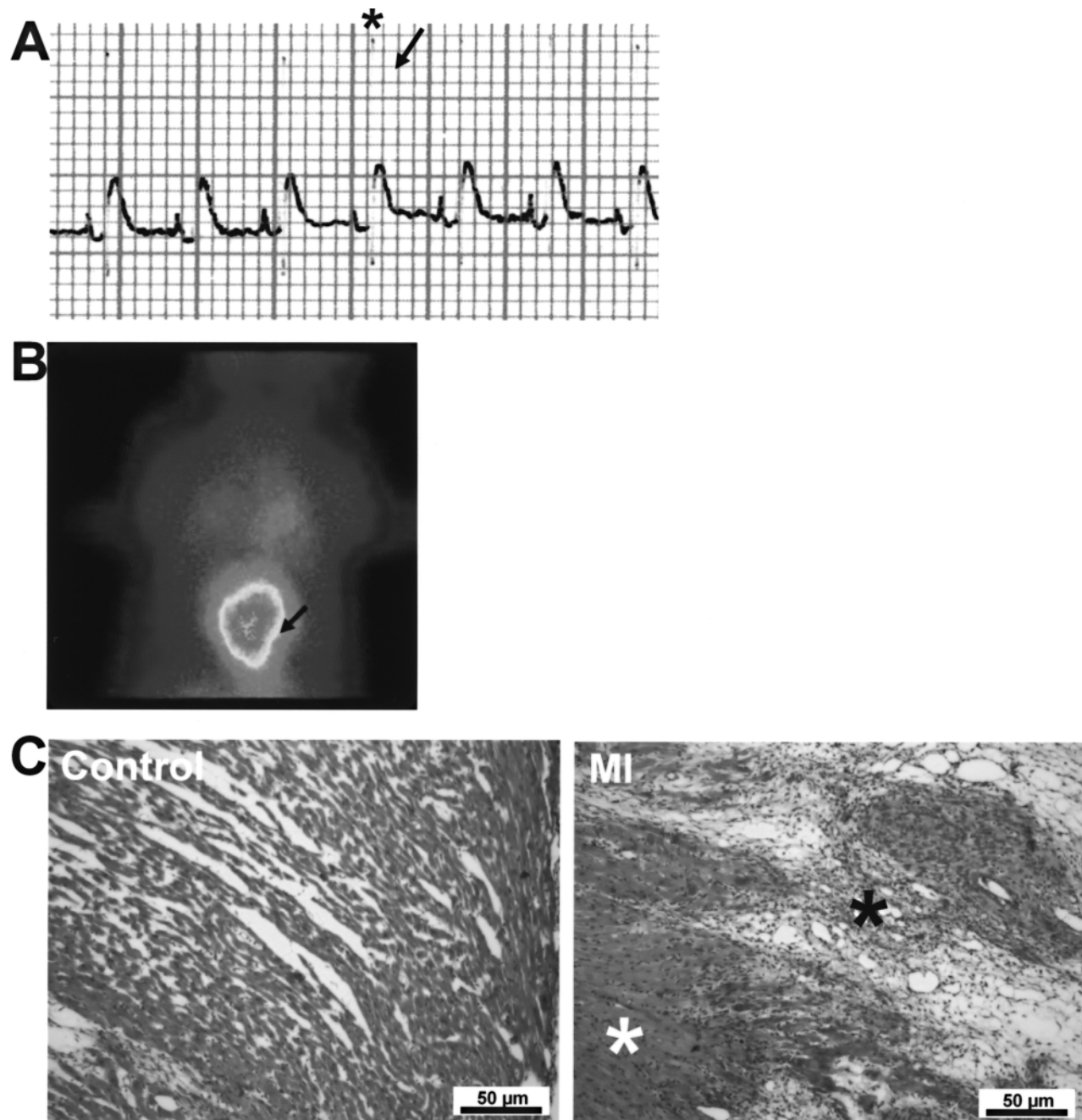


Figure 2. Evaluation of the myocardial infarction protocol. (A) Representative ECG tracing from an infarcted rat obtained immediately after the MI procedure showing elevation of the ST segment (arrow) and an increase in the R wave amplitude (asterisk). (B) Myocardial perfusion scintigraphy using ^{99m}Tc -SESTAMIBI 7 days after MI showed hypocaptation in left ventricle (arrow). (C) Representative photomicrographs of heart slices stained with Masson's trichrome from control and infarcted rats 7 days after MI. White symbols (*) indicate preserved cardiac tissue and black symbol (*) indicates infarcted area.

The number of cells that migrated to infarcted hearts was significantly higher after 5 min of cell injection, as well as during the period of observation (60 min) when compared with sham-operated rats. This effect was apparently specific to the injured tissue because no signifi-

cant changes were observed in other organs such as lungs, kidneys, and spleen. These observations were confirmed by the analysis of isolated organs excised 60 min after injection. In keeping with previous findings, our results indicate that the local microenvironment is

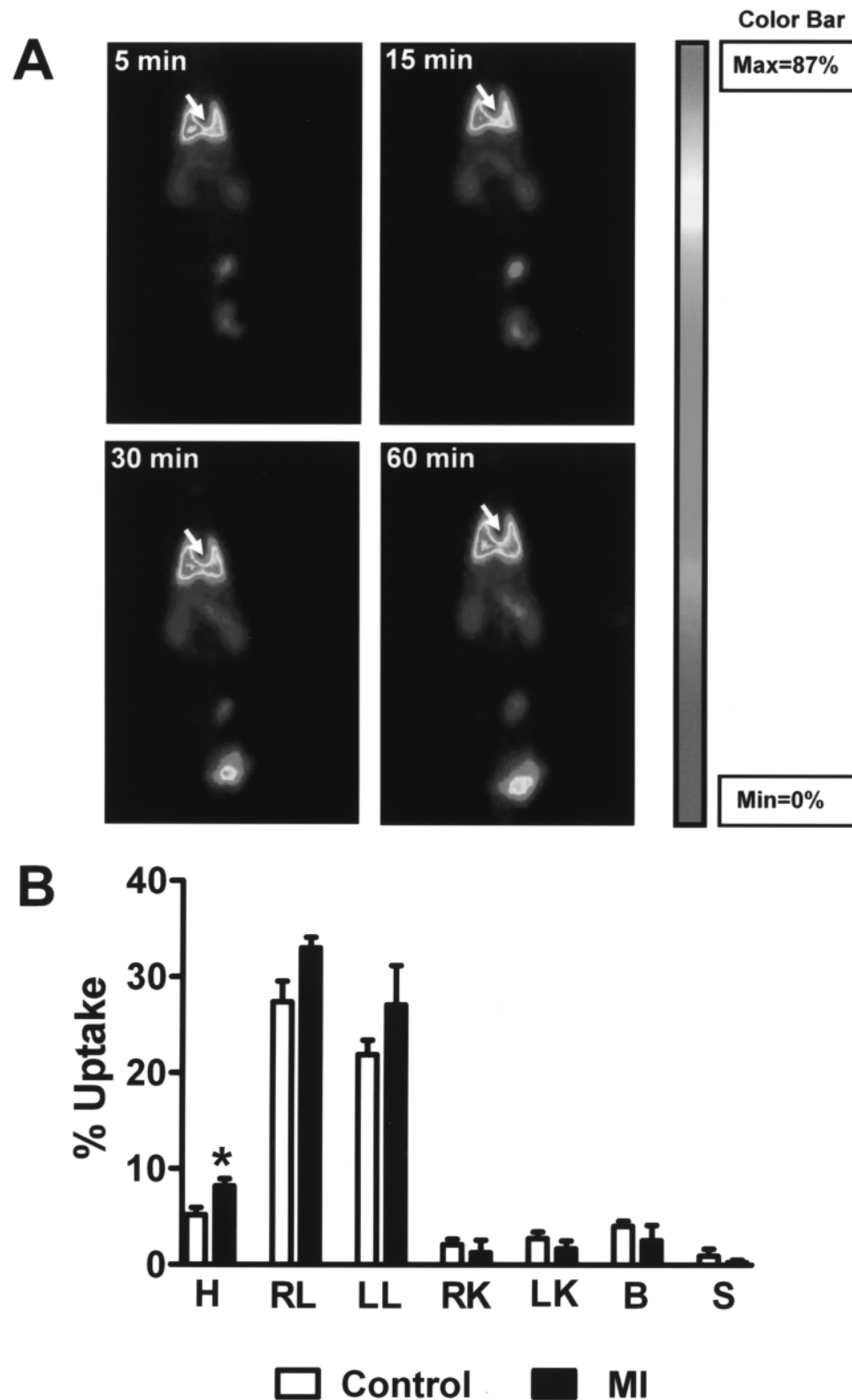


Figure 3. Body distribution of intravenously injected BM-MSCs. (A) Representative scintilography of infarcted rat after ^{99m}Tc -HMPAO-labeled cells injection. The arrow indicates the cardiac area. The cells were found in lungs, heart, kidneys, bladder, and spleen. (B) Quantitative analysis of the body distribution of ^{99m}Tc -HMPAO-labeled cells 5 min after intravenous injection in control and infarcted rats. Data are shown as mean \pm SEM. * $p < 0.05$ versus control hearts (Student t -test). H, heart; RL, right lung; LL, left lung; RK, right kidney; LK, left kidney; B, bladder; S, spleen.

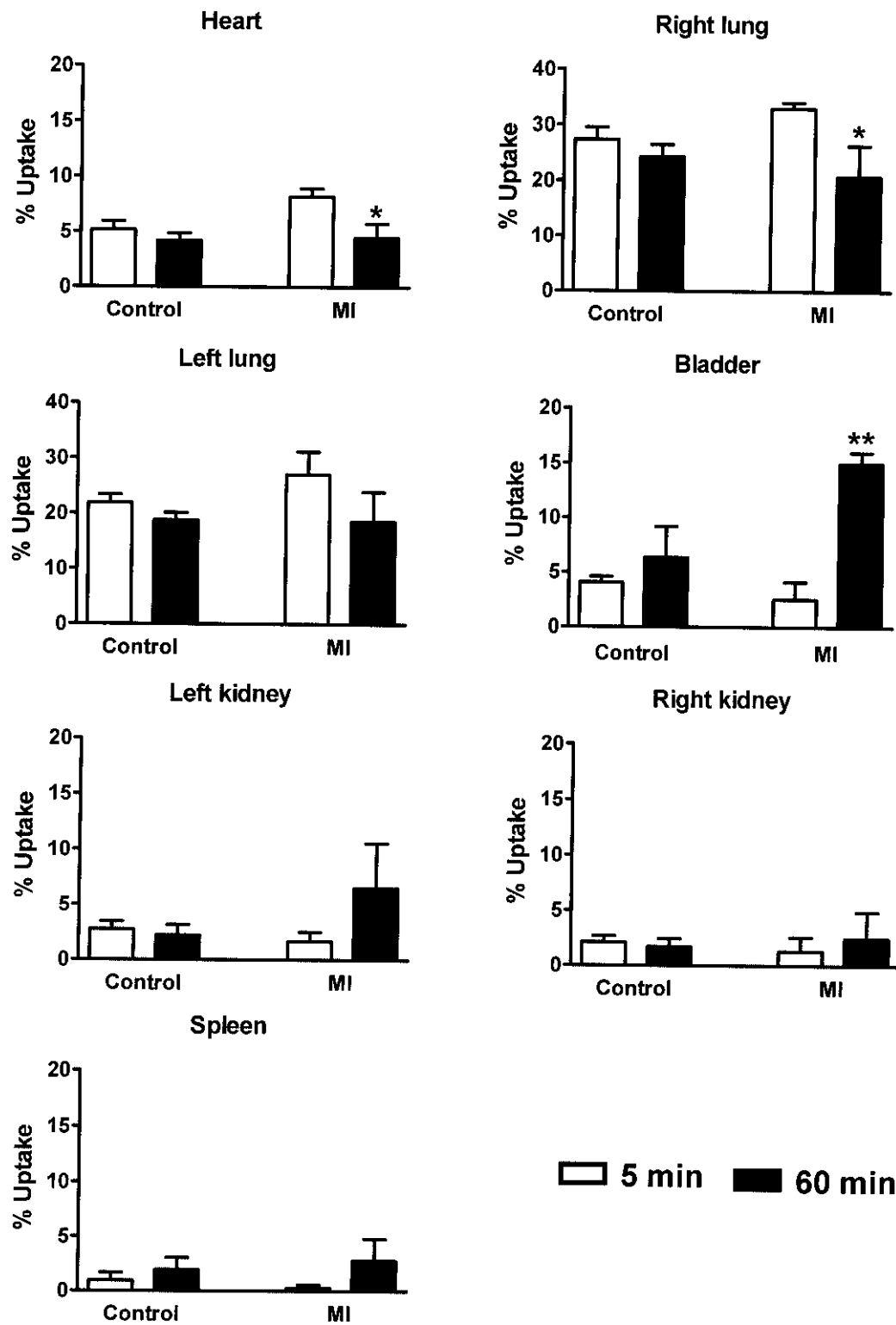


Figure 4. Uptake of BM-MSCs in various organs of control and infarcted animals at 5 and 60 min after cell transplantation. The amount of cells decreased in hearts and right lungs and increased in bladders of MI rats after 60 min of cell injection. Data are shown as mean \pm SEM. * $p < 0.05$ and ** $p < 0.01$ versus 5 min (Student t -test).

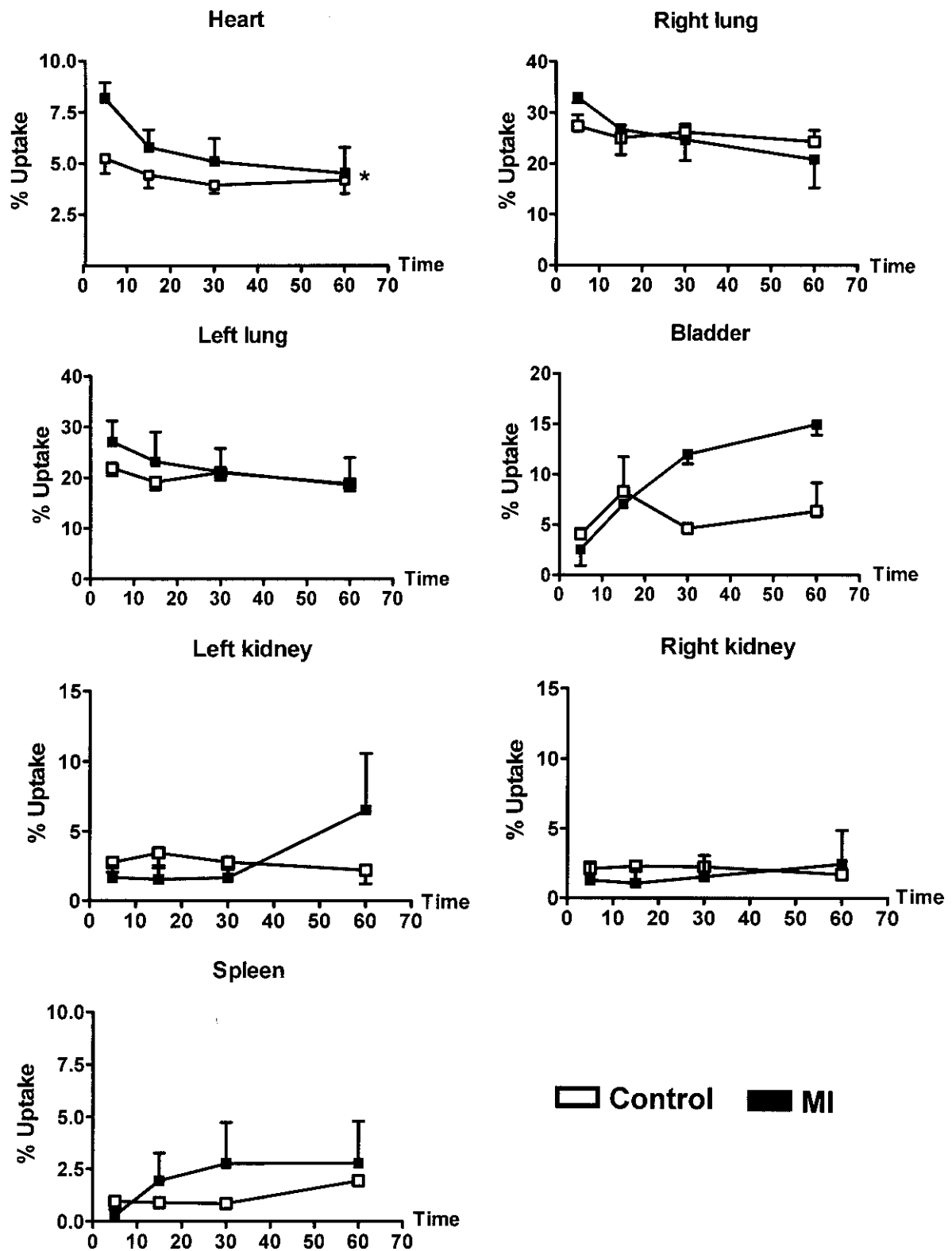


Figure 5. Time course of the distribution of intravenously delivered BM-MSCs in different organs of control and infarcted rats. MI procedure increased the amount of cells in the heart during the period of observation. Data are shown as mean \pm SEM. * $p < 0.05$ versus control hearts (two-way ANOVA followed by the Bonferroni test).

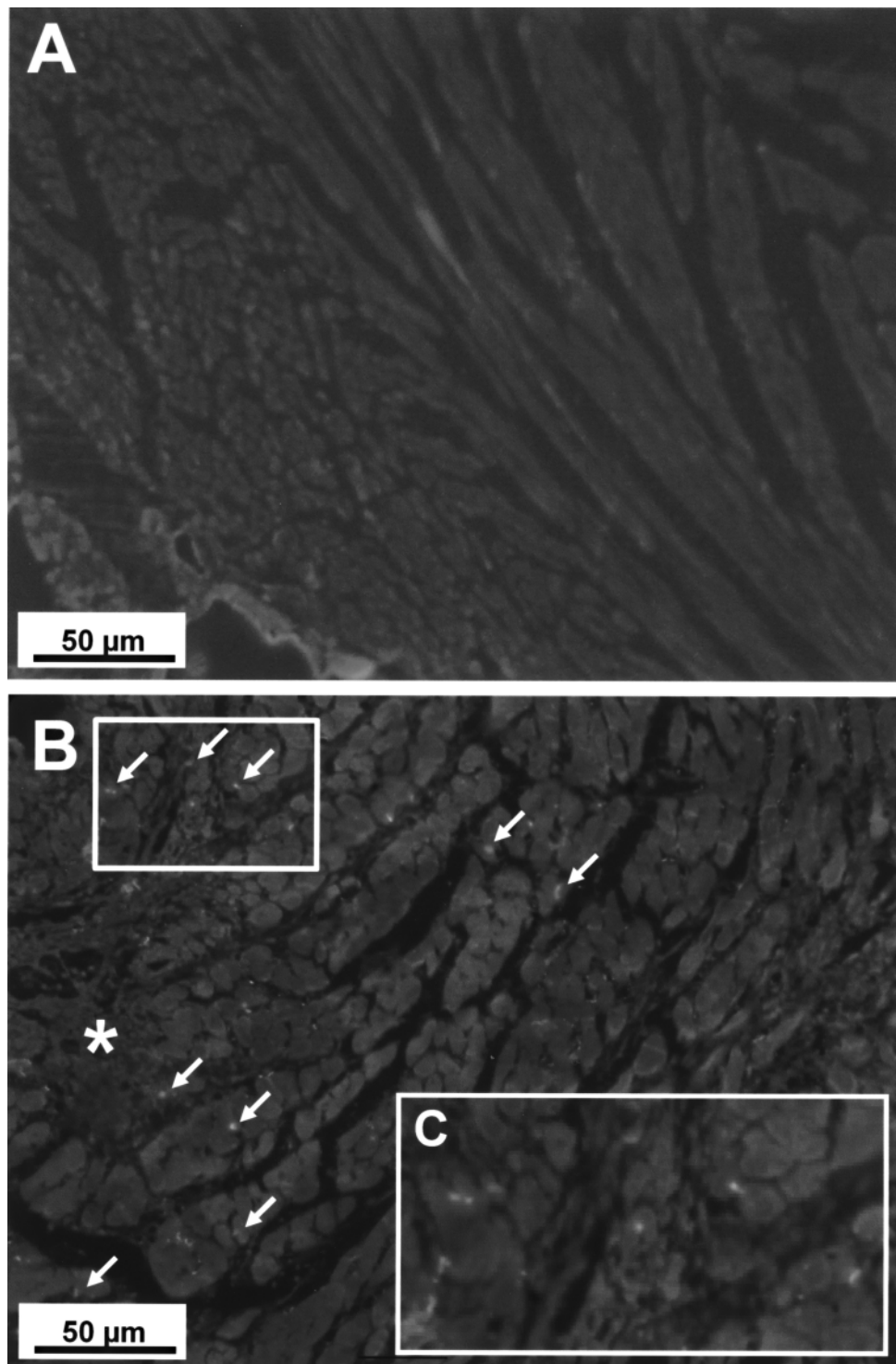


Figure 6. Representative photomicrographs of (A) control and (B) infarcted heart sections of rats injected with DAPI-labeled cells after 7 days of MI. The cells were observed only in infarcted hearts (arrows) and localized in the board of the infarct area (asterisk). (C) The insert represents an amplification of the DAPI-labeled cells area highlighted in (B).

important to guide the homing process because it might express specific receptors and/or chemoattractant factors that facilitate the trafficking, adhesion, and infiltration of BM-MSCs in the injury site (6,9).

Interestingly, the number of cells in ischemic hearts decreased 60 min after inoculation when compared with the first time point of analysis (5 min) ($p < 0.05$ and power of the test = 80.3%). Considering that cardiac function is improved in rats treated with BM-MSCs (16,30,31,36), our observations suggest that the beneficial effects induced by BM-MSCs are not caused by the cells per se, but it is induced by a yet unidentified factor secreted by these cells in the infarcted area and/or by cardiac factors or cells activated by the BM-MSCs. In fact, the mechanisms of action by which BM-MSCs induce their cardioprotective effects are not fully understood. Thus, it has been proposed that the BM-MSCs can differentiate into cardiomyocytes in the injured area, secrete biochemical factors that could activate local protective mechanisms, directly influence the reparative process, or even promote heart repair by a combination of these factors (33).

^{99m}Tc-HMPAO-labeled BM-MSCs were found mainly in the lungs (~70%) both in control and infarcted rats at 5 min of cell injection and, in injured hearts, the number of cells decreased after 60 min in the lungs. Thus, in accordance with previous reports, systemic intravenous delivery of BM-MSCs after MI, although feasible, is limited by entrapment of the cells in the lungs (1). The entrapment of expanded BM-MSCs in the lungs could be explained by their relatively large size (15–19 μ m) and expression of adhesion molecules in the cell membranes. As a result, they may not be able to pass through lung capillaries and many of them become trapped. Accordingly, Schrepfer et al. (28) demonstrated that the nitric oxide donor sodium nitroprusside increases the cell passage through lung capillaries and reduces the cell trapping in mice. However, we cannot rule out the possibility that the surgical procedure or even the MI produced lung injuries that contributed to the entrapment of the infused cells in lungs. Furthermore, the presence of cells in the kidneys and spleen indicates that these organs are also barriers for the infused cells on their homing to infarcted myocardium. The increase of radioactivity levels in the bladder could be explained by urinary excretion of the lipophilic complex (^{99m}Tc-HMPAO) (37).

In summary, these results indicate that the migration of systemically delivered BM-MSCs to infarcted hearts is time dependent and that MI specifically increases the homing of BM-MSCs to the injured areas. However, this approach is limited by cell entrapment in the lungs. Moreover, our findings suggest that a better understanding of the kinetic of migration and distribution of the

BM-MSCs is crucial to enhance the therapeutic potential of these cells in tissue repair.

ACKNOWLEDGMENTS: *The authors thank the Ecograf Núcleo de Diagnóstico Cardiovascular S/C Ltda-Santa Efigênia for kindly providing technetium-99m. This study was supported in part by CNPq (Conselho Nacional de Desenvolvimento Científico e Tecnológico), CAPES (Coordenação de Aperfeiçoamento de Pessoal de Nível Superior), and FAPEMIG (Fundação de Amparo à Pesquisa do Estado de Minas Gerais).*

REFERENCES

1. Barbash, I. M.; Chouraqui, P.; Baron, J.; Feinberg, M. S.; Etzion, S.; Tessone, A.; Miller, L.; Guetta, E.; Zipori, D.; Kedes, L. H.; Kloner, R. A.; Leor, J. Systemic delivery of bone marrow-derived mesenchymal stem cells to the infarcted myocardium: Feasibility, cell migration, and body distribution. *Circulation* 108:863–868; 2003.
2. Barthel, H.; Kämpfer, I.; Seese, A.; Dannenberg, C.; Kluge, R.; Burchert, W.; Knapp, W. H. Improvement of brain SPECT by stabilization of Tc-99m-HMPAO with methylene blue or cobalt chloride. *Nuklearmedizin* 38:80–84; 1999.
3. Bauersachs, J.; Thum, T.; Frantz, S.; Ertl, G. Cardiac regeneration by progenitor cells bedside before bench? *Eur. J. Clin. Invest.* 35:417–420; 2005.
4. Berridge, M. V.; Tan, A. S. Characterization of the cellular reduction of 3-(4,5-dimethylthiazol-2-yl)-2,5-diphenyltetrazolium bromide (MTT): Subcellular localization, substrate dependence, and involvement of mitochondrial electron transport in MTT reduction. *Arch. Biochem. Biophys.* 303:474–482; 1993.
5. Bianco, P.; Riminucci, M.; Gronthos, S.; Robey, P. G. Bone marrow stromal stem cells: Nature, biology, and potential applications. *Stem Cells* 19:180–192; 2001.
6. Chamberlain, G.; Fox, J.; Ashton, B.; Middleton, J. Concise review: mesenchymal stem cells: Their phenotype, differentiation capacity, immunological features, and potential for homing. *Stem Cells* 25:2739–2749; 2007.
7. Chen, Y.; Shao, J. Z.; Xiang, L. X.; Dong, X. J.; Zhang, G. R. Mesenchymal stem cells: a promising candidate in regenerative medicine. *Int. J. Biochem. Cell Biol.* 40:815–820; 2008.
8. Delorme, B.; Ringe, J.; Gallay, N.; Le Vern, Y.; Kerboeuf, D.; Jorgensen, C.; Rosset, P.; Sensebé, L.; Layrolle, P.; Häupl, T.; Charbord, P. Specific plasma membrane protein phenotype of culture-amplified and native human bone marrow mesenchymal stem cells. *Blood* 111:2631–2635; 2008.
9. Devine, S. M.; Cobbs, C.; Jennings, M.; Bartholomew, A.; Hoffman, R. Mesenchymal stem cells distribute to a wide range of tissues following systemic infusion into nonhuman primates. *Blood* 101:2999–3001; 2003.
10. Dohmann, H. F.; Perin, E. C.; Takiya, C. M.; Silva, G. V.; Silva, S. A.; Sousa, A. L.; Mesquita, C. T.; Rossi, M. I.; Pascarelli, B. M.; Assis, I. M.; Dutra, H. S.; Assad, J. A.; Castello-Branco, R. V.; Drummond, C.; Dohmann, H. J.; Willerson, J. T.; Borojevic, R. Transcatheter autologous bone marrow mononuclear cell injection in ischemic heart failure: Postmortem anatomicopathologic and immunohistochemical findings. *Circulation* 112:521–526; 2005.
11. Dominici, M.; Le Blanc, K.; Mueller, I.; Slaper-Corten-

- bach, I.; Marini, F.; Krause, D.; Deans, R.; Keating, A.; Prockop, D. J.; Horwitz, E. Minimal criteria for defining multipotent mesenchymal stromal cells. The International Society for Cellular Therapy position statement. *Cytherapy* 8:315–317; 2006.
12. Ferreira, A. J.; Jacoby, B. A.; Araújo, C. A.; Macedo, F. A.; Silva, G. A.; Almeida, A. P.; Caliari, M. V.; Santos, R. A. S. The nonpeptide angiotensin-(1-7) receptor Mas agonist AVE 0991 attenuates heart failure induced by myocardial infarction. *Am. J. Physiol. Heart Circ. Physiol.* 292:1113–1119; 2007.
13. Fotakis, G.; Timbrell, J. A. In vitro cytotoxicity assays: Comparison of LDH, neutral red, MTT and protein assay in hepatoma cell lines following exposure to cadmium chloride. *Toxicol. Lett.* 160:171–177; 2006.
14. Friedenstein, A. J. Marrow stromal fibroblasts. *Calcif. Tissue Int.* 56:S17; 1995.
15. Gieni, R. S.; Li, Y.; HayGlass, K. T. Comparison of [3H]thymidine incorporation with MTT- and MTS-based bioassays for human and murine IL-2 and IL-4 analysis. Tetrazolium assays provide markedly enhanced sensitivity. *J. Immunol. Methods* 187:85–93; 1995.
16. Henning, R. J.; Burgos, J. D.; Vasko, M.; Alvarado, F.; Sanberg, C. D.; Sanberg, P. R.; Morgan, M. B. Human cord blood cells and myocardial infarction: Effect of dose and route of administration on infarct size. *Cell Transplant.* 16:907–917; 2007.
17. Jiang, W.; Ma, A.; Wang, T.; Han, K.; Liu, Y.; Zhang, Y.; Dong, A.; Du, Y.; Huang, X.; Wang, J.; Lei, X.; Zheng, X. Homing and differentiation of mesenchymal stem cells delivered intravenously to ischemic myocardium in vivo: A time-series study. *Pflugers Arch.* 453: 43–52; 2006.
18. Kupatt, C.; Hinkel, R.; Lamparter, M.; von Brühl, M. L.; Pohl, T.; Horstkotte, J.; Beck, H.; Müller, S.; Delker, S.; Gildehaus, F. J.; Büning, H.; Hatzopoulos, A. K.; Boekstegers, P. Retroinfusion of embryonic endothelial progenitor cells attenuates ischemia-reperfusion injury in pigs: Role of phosphatidylinositol 3-kinase/AKT kinase. *Circulation* 112:I117–I122; 2005.
19. Lakshminpathy, U.; Hart, R. P. Concise review: MicroRNA expression in multipotent mesenchymal stromal cells. *Stem Cells* 26:356–363; 2008.
20. Machado, C. B.; Ventura, J. M.; Lemos, A. F.; Ferreira, J. M.; Leite, M. F.; Goes, A. M. 3D chitosan-gelatin-chondroitin porous scaffold improves osteogenic differentiation of mesenchymal stem cells. *Biomed. Mater.* 2:124–131; 2007.
21. Mesquita, C. T.; Correa, P. L.; Felix, R. C.; Azevedo, J. C.; Alves, S.; Oliveira, C. C.; Sousa, A. L.; Borojevic, R.; Dohmann, H. F. Autologous bone marrow mononuclear cells labeled with Tc-99m hexamethylpropylene amine oxime scintigraphy after intracoronary stem cell therapy in acute myocardial infarction. *J. Nucl. Cardiol.* 12:610–612; 2005.
22. Mortelmans, L.; Malbrain, S.; Stuyck, J.; De Backer, C.; Heynen, M. J.; Boogaerts, M.; De Roo, M.; Verbruggen, A. In vitro and in vivo evaluation of granulocyte labeling with [99mTc] d,1-HMPAO. *J. Nucl. Med.* 30:2022–2028; 1989.
23. Mosmann, T. Rapid colorimetric assay for cellular growth and survival: Application to proliferation and cytotoxicity assays. *J. Immunol. Methods* 65:55–63; 1983.
24. Neuhuber, B.; Gallo, G.; Howard, L.; Kostura, L.; Mackay, A.; Fischer, I. Reevaluation of in vitro differentiation protocols for bone marrow stromal cells: Disruption of actin cytoskeleton induces rapid morphological changes and mimics neuronal phenotype. *J. Neurosci. Res.* 77: 192–204; 2004.
25. Ocarino, N. M.; Bozzi, A.; Pereira, R. D.; Breyner, N. M.; Silva, V. L.; Castanheira, P.; Goes, A. M.; Serakides, R. Behavior of mesenchymal stem cells stained with 4', 6-diamidino-2-phenylindole dihydrochloride (DAPI) in osteogenic and non osteogenic cultures. *Biocell* 32:175–183; 2008.
26. Pedemonte, E.; Benvenuto, F.; Casazza, S.; Mancardi, G.; Oksenberg, J. R.; Uccelli, A.; Baranzini, S. E. The molecular signature of therapeutic mesenchymal stem cells exposes the architecture of the hematopoietic stem cell niche synapse. *BMC Genomics* 8:65; 2007.
27. Phinney, D. G. Building a consensus regarding the nature and origin of mesenchymal stem cells. *J. Cell. Biochem. Suppl.* 38:7–12; 2002.
28. Schrepfer, S.; Deuse, T.; Reichenspurner, H.; Fischbein, M. P.; Robbins, R. C.; Pelletier, M. P. Stem cell transplantation: The lung barrier. *Transplant. Proc.* 39:573–576; 2007.
29. Sheikh, A. Y.; Lin, S. A.; Cao, F.; Cao, Y.; van der Bogt, K. E.; Chu, P.; Chang, C. P.; Contag, C. H.; Robbins, R. C.; Wu, J. C. Molecular imaging of bone marrow mononuclear cell homing and engraftment in ischemic myocardium. *Stem Cells* 25:2677–2684; 2007.
30. Siepe, M.; Heilmann, C.; Samson, P. V.; Menasché, P.; Beyersdorf, F. Stem cell research and cell transplantation for myocardial regeneration. *Eur. J. Cardiothorac. Surg.* 28:318–324; 2005.
31. Stamm, C.; Liebold, A.; Steinhoff, G.; Strunk, D. Stem cell therapy for ischemic heart disease: Beginning or end of the road? *Cell Transplant.* 15:S47–S56; 2006.
32. Stamm, C.; Nasser, B.; Drews, T.; Hetzer, R. Cardiac cell therapy: A realistic concept for elderly patients? *Exp. Gerontol.* 43:679–690; 2008.
33. Tousoulis, D.; Briasoulis, A.; Antoniadis, C.; Stefanadis, E.; Stefanadis, C. Heart regeneration: What cells to use and how? *Curr. Opin. Pharmacol.* 8:211–218; 2008.
34. Wang, T.; Tang, W.; Sun, S.; Ristagno, G.; Huang, Z.; Weil, M. H. Intravenous infusion of bone marrow mesenchymal stem cells improves myocardial function in a rat model of myocardial ischemia. *Crit. Care Med.* 35:2587–2593; 2007.
35. Yoon, C. H.; Hur, J.; Oh, I. Y.; Park, K. W.; Kim, T. Y.; Shin, J. H.; Kim, J. H.; Lee, C. S.; Chung, J. K.; Park, Y. B.; Kim, H. S. Interleukin-1 is upregulated in ischemic muscle, which mediates trafficking of endothelial progenitor cells. *Arterioscler. Thromb. Vasc. Biol.* 26:1066–1072; 2006.
36. Zhang, S.; Jia, Z.; Ge, J.; Gong, L.; Ma, Y.; Li, T.; Guo, J.; Chen, P.; Hu, Q.; Zhang, P.; Liu, Y.; Li, Z.; Ma, K.; Li, L.; Zhou, C. Purified human bone marrow multipotent mesenchymal stem cells regenerate infarcted myocardium in experimental rats. *Cell Transplant.* 14:787–798; 2005.
37. Zhou, R.; Thomas, D. H.; Qiao, H.; Bal, H. S.; Choi, S. R.; Alavi, A.; Ferrari, V. A.; Kung, H. F.; Acton, P. D. In vivo detection of stem cells grafted in infarcted rat myocardium. *J. Nucl. Med.* 45:816–822; 2005.